






## RESISTIVE SWITCHING BEHAVIOR OF $\text{SnO}_2/\text{ZnO}$ HETEROJUNCTION THIN FILMS FOR NON-VOLATILE MEMORY APPLICATIONS

 Jamoliddin X. Murodov<sup>a,b\*</sup>,  Shavkat U. Yuldashev<sup>b</sup>,  Azamat O. Arslanov<sup>c</sup>, Noiba U. Botirova<sup>b</sup>,  
 Javohir Sh. Xudoyqulov<sup>c,e</sup>, Ra'no Sh. Sharipova<sup>b</sup>, Rafael A. Nusretov<sup>a</sup>, Andrey A. Nebesniy<sup>c</sup>,  
 Mukhammad P. Pirimmatov<sup>d</sup>

<sup>a</sup>Tashkent State Technical University named after Islam Karimov, Tashkent, Uzbekistan

<sup>b</sup>Center of Nanotechnology Development, National University of Uzbekistan, Tashkent, Uzbekistan

<sup>c</sup>National University of Uzbekistan named after Mirzo Ulugbek, Tashkent, Uzbekistan

<sup>d</sup>Institute of Physics and Technology, Tashkent, Uzbekistan

<sup>e</sup>Central Asian University, Tashkent, Uzbekistan

\*Corresponding Author E-mail: [jamoliddinmilliy@gmail.com](mailto:jamoliddinmilliy@gmail.com)

Received June 3, 2025, revised July 3, 2025; accepted August 8, 2025

This study presents the fabrication and resistive switching (RS) performance of bilayer  $\text{SnO}_2/\text{ZnO}$  thin films deposited via ultrasonic spray pyrolysis on p-type silicon substrates. The heterostructures were post-annealed at 450°C to enhance crystallinity and interfacial contact. Electrical characterization using I–V measurements revealed clear bipolar RS behavior without the need for an initial forming process. The devices exhibited a stable high resistance state (HRS) and low resistance state (LRS) across multiple cycles, with an ON/OFF ratio exceeding  $10^2$ . The switching mechanism is attributed to the formation and rupture of conductive filaments likely induced by oxygen vacancies at the  $\text{SnO}_2/\text{ZnO}$  interface. Bandgap estimation using Tauc plots showed values of approximately 3.17 eV and 3.41 eV for ZnO and  $\text{SnO}_2$ , respectively. These findings confirm the potential of  $\text{SnO}_2/\text{ZnO}$  heterojunctions as efficient materials for next-generation non-volatile memory applications.

**Keywords:**  $\text{SnO}_2$ ; ZnO; Resistive switching; Memristor; Thin films; Heterojunction; Non-volatile memory; Oxygen vacancies

**PACS:** 73.40.-c; 85.30 Tv; 73.6 Ga

### INTRODUCTION

In recent years, memristors have become a highly relevant research topic due to their potential in neuromorphic computing, artificial intelligence hardware, and next-generation non-volatile memory systems. Memristors are considered the fourth fundamental passive circuit element—alongside resistors, capacitors, and inductors—and are capable of remembering their resistance state based on the history of electrical charge passed through them. This unique feature enables memristors to retain information even when the power is turned off, making them ideal candidates for low-power, high-density memory devices [1-3].

Metal oxide-based memristors, particularly those formed from binary oxides such as ZnO and  $\text{SnO}_2$ , have drawn substantial interest due to their low fabrication cost, ease of synthesis, and compatibility with flexible substrates. Both ZnO and  $\text{SnO}_2$  are wide-bandgap n-type semiconductors, with bandgaps of approximately 3.4 eV and 3.6 eV, respectively. ZnO offers high electron mobility and good surface reactivity, while  $\text{SnO}_2$  is chemically stable and exhibits strong electrical conductivity in its doped forms [4,5]. Combining these materials into a bilayer or heterojunction structure can enable new resistive switching mechanisms, such as interface-modulated filament formation and oxygen vacancy migration.

Prior investigations by Pant et al. [6] have revealed strong bipolar resistive switching and pronounced negative differential resistance (NDR) characteristics in  $\text{SnO}_2/\text{ZnO}$  heterojunctions synthesized via magnetron sputtering. These effects were attributed to enhanced grain boundary diffusion and the emergence of quantum confinement phenomena at the nanoscale interface. In a more recent study, Saha et al. [7] demonstrated reliable resistive switching in one-dimensional  $\text{SnO}_2$  nanofiber-based memristors, where switching dynamics were effectively analyzed and predicted using artificial neural network (ANN)-based computational models, further supporting the applicability of data-driven approaches in oxide-based memory device engineering. Furthermore, Co-doped  $\text{SnO}_2$  memristors fabricated on p-type silicon substrates have been shown to exhibit tunable negative differential resistance behavior, highlighting the role of doping in modulating the electronic properties of oxide-based heterostructures [8].

In this study, we investigate the resistive switching behavior of a p-Si/ $\text{SnO}_2/\text{ZnO}$  heterostructure fabricated using ultrasonic spray pyrolysis (USP), an accessible and scalable thin-film deposition technique. The  $\text{SnO}_2$  and ZnO layers were sequentially deposited on both p-type silicon and quartz substrates, with post-annealing at 450°C. Current–voltage (I–V) measurements were performed using a Keithley 2460 SourceMeter. The results show a clear hysteresis loop, indicative of memristive switching. However, the relatively close bandgap values of ZnO and  $\text{SnO}_2$  may limit the strength of the switching contrast, as both layers are n-type semiconductors. This study contributes to the ongoing effort to optimize binary oxide heterojunctions for low-power memory devices.

**Cite as:** J.X. Murodov, Sh.U. Yuldashev, A.O. Arslanov, N.U. Botirova, J.Sh. Xudoyqulov, R.Sh. Sharipova, R.A. Nusretova, A.A. Nebesniy, M.P. Pirimmatov, East Eur. J. Phys. 3, 348 (2025), <https://doi.org/10.26565/2312-4334-2025-3-34>

© J.X. Murodov, Sh.U. Yuldashev, A.O. Arslanov, N.U. Botirova, J.Sh. Xudoyqulov, R.Sh. Sharipova, R.A. Nusretova, A.A. Nebesniy, M.P. Pirimmatov, 2025; CC BY 4.0 license

## METHODS

The p-Si/ $\text{SnO}_2$ / $\text{ZnO}$  heterostructure thin films were fabricated using the ultrasonic spray pyrolysis (USP) technique due to its cost-effectiveness, simplicity, and suitability for oxide thin film deposition. In this study, p-type silicon substrates were used. Prior to deposition, the substrates were cleaned sequentially by rinsing in deionized (DI) water, followed by ethanol and then acetone, and finally rinsed again in DI water. This multi-step cleaning process was performed to remove organic and inorganic contaminants and to ensure uniform and adherent film growth. After cleaning, the substrates were dried naturally under ambient laboratory conditions.

The schematic structure of the fabricated memristor device is illustrated in Figure 1. The device consists of a bilayer  $\text{SnO}_2$ / $\text{ZnO}$  heterostructure deposited on a p-type silicon substrate. Silver (Ag) top contacts were applied as electrodes. The  $\text{ZnO}$  layer serves as the intermediate interface layer, while  $\text{SnO}_2$  is the top oxide layer. The bottom electrode is the p-Si substrate itself. This vertical "sandwich-like" configuration enables charge transport across the oxide layers under applied bias, which is essential for studying resistive switching behavior.

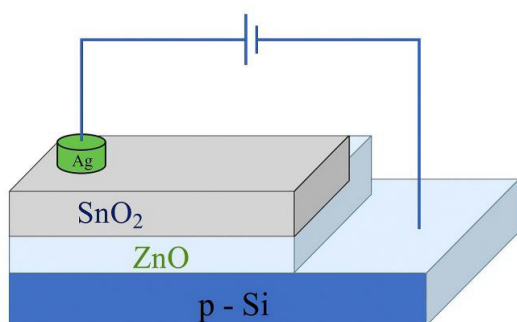


**Figure 1.** Schematic illustration of the Ag/ $\text{SnO}_2$ / $\text{ZnO}$ /p-Si memristor device structure

After the chemical cleaning steps, the substrates were rinsed thoroughly with deionized (D.I.) water to remove any remaining traces of solvents and impurities. Finally, the cleaned substrates were dried using nitrogen gas. This multi-step cleaning process was crucial for achieving a uniform film morphology and ensuring reproducible electrical performance of the memristor devices. Compared to a simple rinse method, this procedure significantly reduced surface contamination, thereby improving the quality and reproducibility of the  $\text{SnO}_2$  and  $\text{ZnO}$  films deposited via ultrasonic spray pyrolysis (USP) [9].

The  $\text{SnO}_2$  precursor solution was prepared by dissolving 15 mL of stannous chloride dihydrate ( $\text{SnCl}_2 \cdot 2\text{H}_2\text{O}$ ) in double-distilled water. For the  $\text{ZnO}$  layer, 15 mL of zinc acetate dihydrate [ $\text{Zn}(\text{C}_2\text{H}_3\text{O}_2)_2 \cdot 2\text{H}_2\text{O}$ ] was similarly dissolved in double-distilled water. Each solution was atomized using a 2.5 MHz

ultrasonic transducer and carried toward the heated substrates using oxygen gas as the carrier.

The deposition process was conducted at a substrate temperature of  $450^\circ\text{C}$ , which was maintained using a controlled hotplate. The  $\text{SnO}_2$  layer was deposited first, followed by the  $\text{ZnO}$  layer, forming a bilayer heterostructure. This sequence was designed to promote appropriate band alignment and interfacial contact between the n-type semiconductors. Following deposition, the films were annealed in ambient air at  $450^\circ\text{C}$  to improve crystallinity and stabilize the interface. Silver (Ag) top contacts were applied using silver paste for electrical measurements, and the p-Si substrate served as the bottom electrode in the case of silicon-based structures.

Electrical characterization of the memristor devices was performed using a Keithley 2460 SourceMeter. A voltage sweep protocol of  $0 \rightarrow +5\text{ V} \rightarrow 0 \rightarrow -5\text{ V} \rightarrow 0$  was applied to examine the current–voltage (I–V) characteristics. The presence of a hysteresis loop in the I–V curve confirmed the resistive switching behavior of the fabricated structures.

## RESULTS

### A. Current–Voltage (I–V) Characteristics

The electrical response of the p-Si/ $\text{SnO}_2$ / $\text{ZnO}$  heterostructure was evaluated through current–voltage (I–V) measurements using a Keithley 2460 SourceMeter. A voltage sweep in the range of  $0 \rightarrow +5\text{ V} \rightarrow 0 \rightarrow -5\text{ V} \rightarrow 0$  was applied. As shown in Figure 2, the device exhibits a pronounced hysteresis loop, which is characteristic of bipolar resistive switching behavior. Notably, the switching occurred without the requirement of an initial forming voltage, suggesting the presence of intrinsic defect states – most likely oxygen vacancies – within the oxide layers that facilitate the conductive filament formation.

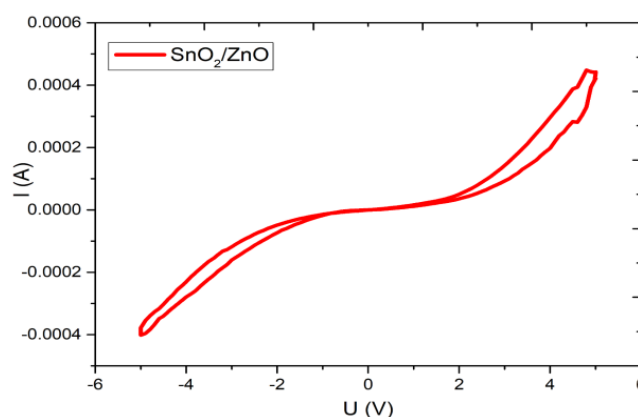


**Figure 2.** Linear-scale I–V characteristics of the  $\text{SnO}_2$ / $\text{ZnO}$  heterostructure, showing memristive switching.

This behavior is consistent with the findings of Pant et al. [6], who observed similar bipolar switching in SnO<sub>2</sub>/ZnO interfaces attributed to the diffusion of ZnO into SnO<sub>2</sub> at the grain boundaries, forming a resonant tunneling-like interface. The observed switching behavior here can be explained by the formation and rupture of conductive filaments in the oxide layers, likely modulated by the applied electric field and the associated drift of oxygen vacancies.

However, due to the small bandgap difference between ZnO (~3.4 eV) and SnO<sub>2</sub> (~3.6 eV), and the fact that both are n-type semiconductors, the overall barrier height at the interface may be low. As a result, the current contrast between the high resistance state (HRS) and the low resistance state (LRS) is moderate, though stable. The ON/OFF current ratio was estimated to be >10<sup>2</sup>, which is suitable for low-power memory applications.

### B. Optical Bandgap Estimation

The optical bandgaps of the individual ZnO and SnO<sub>2</sub> layers were estimated using Tauc plot analysis derived from UV-Vis absorbance spectra (see Figure 3). By plotting  $(\alpha h\nu)^2$  versus photon energy ( $h\nu$ ) and extrapolating the linear region to the energy axis, the direct bandgap values were determined. The estimated optical bandgaps were found to be approximately: ZnO layer (3.17 eV), SnO<sub>2</sub> layer (3.41 eV)

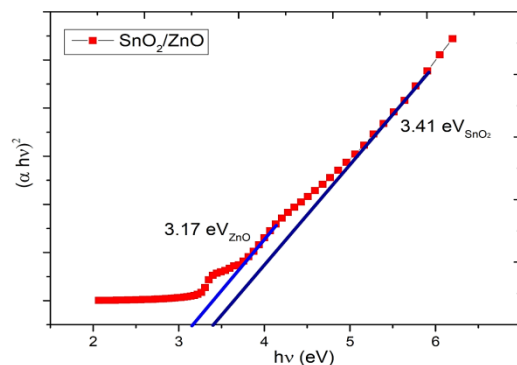


**Figure 3.** Tauc plot used for bandgap estimation of ZnO (3.17 eV) and SnO<sub>2</sub> (3.41 eV)

These values closely match literature-reported data [6,7], confirming the successful synthesis of phase-pure oxide layers. The slight narrowing of the SnO<sub>2</sub> bandgap compared to the nominal 3.6 eV may be attributed to oxygen vacancy-related subgap states, which can affect the switching performance by serving as electron trapping centers.

### C. Structural Characterization (XRD Analysis)

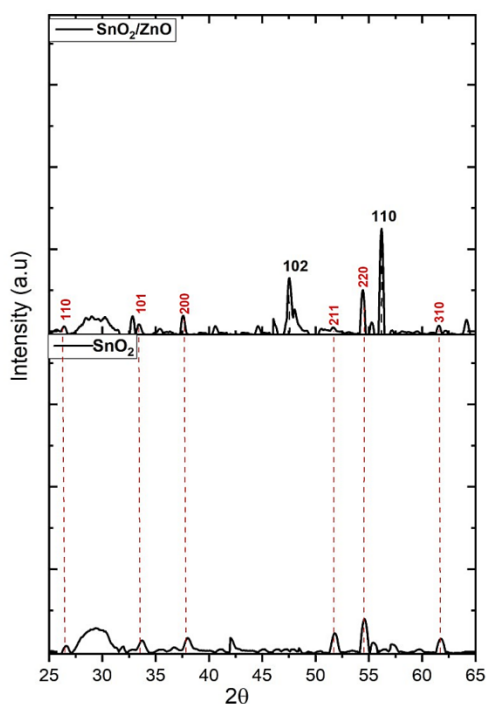


**Figure 4.** XRD pattern of the SnO<sub>2</sub>/ZnO heterojunction thin film

The crystallographic properties of the synthesized SnO<sub>2</sub>/ZnO bilayer thin films were investigated using X-ray diffraction (XRD). Figure 4 presents the XRD pattern of the heterostructure deposited on a p-type Si substrate. The diffraction peaks observed at  $2\theta \approx 31.7^\circ$ ,  $34.4^\circ$ ,  $36.2^\circ$ ,  $47.5^\circ$ ,  $56.6^\circ$ , and  $62.8^\circ$  are assigned to the (100), (002), (101), (102), (110), and (103) planes of hexagonal wurtzite ZnO, respectively (JCPDS Card No. 36-1451). Additional peaks located at approximately  $26.6^\circ$ ,  $33.9^\circ$ ,  $37.9^\circ$ ,  $51.7^\circ$ , and  $54.8^\circ$  correspond to the (110), (101), (200), (211), and (220) planes of the tetragonal rutile phase of SnO<sub>2</sub> (JCPDS Card No. 41-1445).

These results confirm the successful formation of a polycrystalline bilayer structure containing both ZnO and SnO<sub>2</sub> phases without detectable secondary impurities. The predominance of ZnO peaks is attributed to its top-layer placement in the heterostructure, which contributes to stronger X-ray signal intensity. The sharp and well-defined diffraction peaks indicate good crystallinity, while the absence of unidentified peaks affirms the high phase purity of the deposited films.

The confirmed crystallographic structure supports the electrical measurements, as high crystallinity and structural integrity at the interface are known to influence the stability and reproducibility of resistive switching behavior. The SnO<sub>2</sub>/ZnO heterointerface, therefore, provides a favorable platform for the formation and rupture of conductive filaments, modulated by oxygen vacancy migration, as discussed in the preceding electrical characterization section.

### D. Mechanism Interpretation

The resistive switching mechanism in this heterostructure is likely governed by oxygen vacancy migration and associated filament formation at the  $\text{SnO}_2/\text{ZnO}$  interface. When a positive bias is applied, oxygen ions drift away from the anode, leaving behind oxygen vacancies that accumulate to form conductive paths (filaments). The application of a reverse bias disrupts these paths, returning the device to the high-resistance state.

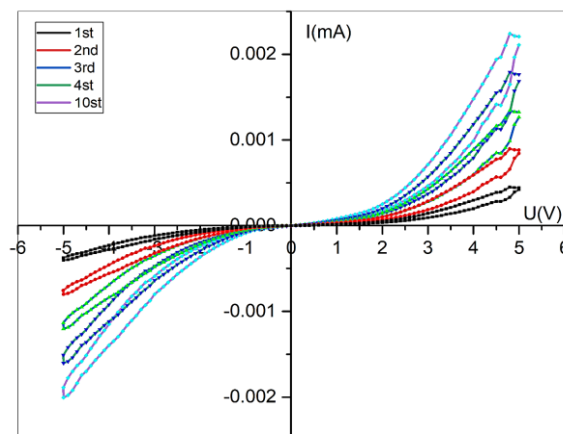


**Figure 5.** Multi-cycle I–V measurements demonstrating reproducibility and stability of resistive switching behavior

Figure 5 shows multi-cycle I–V measurements, clearly demonstrating the reproducibility and stability of the resistive switching behavior over several cycles. The overlapping hysteresis loops indicate consistent switching between high-resistance and low-resistance states, confirming the non-volatile nature and endurance of the memristor device.

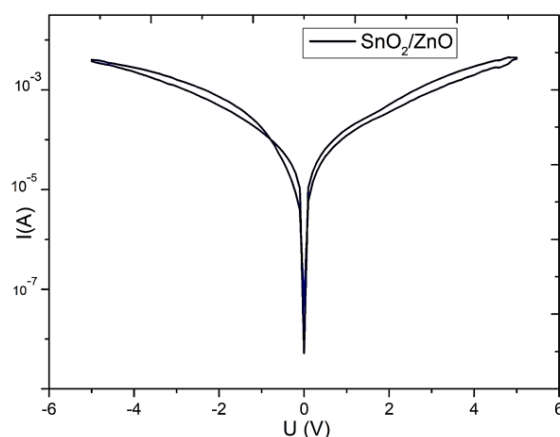


**Figure 6.** Log-scale I–V curve showing clear bipolar switching characteristics of the  $\text{SnO}_2/\text{ZnO}$  heterojunction

Figure 6 presents the log-scale I–V characteristics of the  $\text{SnO}_2/\text{ZnO}$  heterojunction device. The plot clearly illustrates the bipolar switching behavior, with distinct transitions between the high-resistance and low-resistance states under opposite bias polarities. This logarithmic representation helps to highlight the exponential nature of current conduction and the stability of the switching behavior across several orders of magnitude.

The heterointerface, supported by a p-type Si substrate, may also induce additional band bending or depletion effects, modulating the switching threshold. Although both oxide layers are n-type, their slightly different work functions and bandgaps still create an asymmetric potential barrier that contributes to the observed resistive switching (RS) behavior.

### CONCLUSION

In this study, a p-Si/ $\text{SnO}_2/\text{ZnO}$  heterojunction thin film was successfully fabricated using the ultrasonic spray pyrolysis technique. The electrical analysis of the device revealed clear bipolar resistive switching behavior with a stable hysteresis loop observed in the I–V characteristics. The switching occurred without the requirement for a forming step, suggesting that oxygen vacancies and interface effects play a critical role in the RS mechanism.

Tauc plot analysis showed that the optical bandgaps of ZnO and  $\text{SnO}_2$  were approximately 3.17 eV and 3.41 eV, respectively, consistent with reported values in the literature. Although the small band offset between the two n-type oxides may reduce the overall switching contrast, the device demonstrated repeatable ON/OFF cycles and reasonable resistance state separation.

These findings confirm that the p-Si/SnO<sub>2</sub>/ZnO heterostructure is a viable platform for exploring low-cost, oxide-based memristors. Future studies may focus on interface engineering, doping, or inclusion of buffer layers to enhance RS characteristics and device scalability for neuromorphic and non-volatile memory applications.

## ORCID

©Jamoliddin X. Murodov, <https://orcid.org/0009-0006-3088-4881>; ©Shavkat U. Yuldashev, <https://orcid.org/0000-0002-2187-5960>;  
©Azamat O. Arslanov, <https://orcid.org/0009-0000-4817-8770>; ©Mukhammad P. Pirimmatov, <https://orcid.org/0009-0000-4829-7817>;  
©Javohir Sh. Xudoyqulov, <https://orcid.org/0009-0005-4223-8863>

## REFERENCES

- [1] D. Ielmini, "Resistive switching memories based on metal oxides: Mechanisms, reliability and scaling," *Semiconductor Science and Technology*, **31**(6), 063002 (2016). <https://doi.org/10.1088/0268-1242/31/6/063002>
- [2] B. Cao, H. Liu, T. Li, J. Gong, S. Zhang, and M.T. Dove, "Synthesis of composite films for ZnO-based memristors with superior stability," *Materials Research Express*, **11**, 056302 (2024). <https://doi.org/10.1088/2053-1591/ad4777>
- [3] P.D. Walke, *et al.*, "Memristive Devices from CuO Nanoparticles," *Nanomaterials*, **10**(9), 1677 (2020). <https://doi.org/10.3390/nano10091677>
- [4] P.A. Hind, P. Kumar, U.K. Goutam, and B.V. Rajendra, "Impact of deposition temperature on persistent photoconductivity of SnO<sub>2</sub> thin films deposited using spray pyrolysis technique suitable in optoelectronic synaptic devices," *Optical Materials*, **146**, 115579 (2024). <https://doi.org/10.1016/j.optmat.2024.115579>
- [5] N.U. Rehman, R. Khan, N. Rahman, I. Ahmad, A. Ullah, M. Sohail, S. Iqbal, *et al.*, "Dual-doped ZnO-based magnetic semiconductor resistive switching response for memristor-based technologies," *Journal of Materials Science: Materials in Electronics*, **35**, 1557 (2024). <https://doi.org/10.1007/s10854-024-13318-5>
- [6] R. Pant, N. Patel, K.K. Nanda, and S.B. Krupanidhi, "Negative differential resistance and resistive switching in SnO<sub>2</sub>/ZnO interface," *Journal of Applied Physics*, **122**(12), (2017). <https://doi.org/10.1063/1.5004969>
- [7] S. Saha, *et al.* "Experimental demonstration of SnO<sub>2</sub> nanofiber-based memristors and their data-driven modeling for nanoelectronic applications," *Chip*, **2**, 100075 (2023). <https://doi.org/10.1016/j.chip.2023.100075>
- [8] J.X. Murodov, Sh.U. Yuldashev, M.S. Mirkamilova, and U.E. Jurayev, "Tunable Negative Differential Resistance in SnO<sub>2</sub>:Co Memristors on p-Si," *East European Journal of Physics*, (2), 211-214 (2025). <https://doi.org/10.26565/2312-4334-2025-2-22>
- [9] A. Arslanov, Sh. Yuldashev, N. Botirova, R. Nusretov, J. Murodov, and J. Xudoyqulov, "Impact of precursor molar concentration on the structural and optical properties of ZnO thin films synthesized by ultrasonic spray pyrolysis," *Physical Science International Journal*, **29**(1), 29–35 (2025). <https://doi.org/10.9734/psij/2025/v29i1871>

**РЕЗИСТИВНА ПЕРЕМІКАЛЬНА ПОВЕДІНКА ТОНКОПЛІВКОВОГО ГЕТЕРОПЕРЕХОДУ SnO<sub>2</sub>/ZnO  
ДЛЯ ЗАСТОСУВАНЬ В ЕНЕРГОНЕЗАЛЕЖНІЙ ПАМ'ЯТІ**

Джамоліддін Х. Муродов<sup>a,b</sup>, Шавкат У. Юлдашев<sup>b</sup>, Азамат О. Арсланов<sup>c</sup>, Нойба У. Ботірова<sup>b</sup>,  
Джавохір Ш. Худойкулов<sup>c,e</sup>, Рано Ш. Шаріпова<sup>b</sup>, Рафаель А. Нусретов<sup>a</sup>, Андрій А. Небесний<sup>c</sup>,  
Мухаммад П. Пірімматов<sup>d</sup>

<sup>a</sup>Ташкентський державний технічний університет імені Іслама Карімова, Ташкент, Узбекистан

<sup>b</sup>Центр розвитку нанотехнологій, Національний університет Узбекистану, Ташкент, Узбекистан

<sup>c</sup>Національний університет Узбекистану імені Мірзо Улугбека, Ташкент, Узбекистан

<sup>d</sup>Інститут фізики та технологій, Ташкент, Узбекистан

<sup>e</sup>Центральноазіатський університет, Ташкент, Узбекистан

У цьому дослідженні представлено виготовлення та властивості резистивного перемикачання (РС) двошарових тонких плівок SnO<sub>2</sub>/ZnO, нанесених за допомогою ультразвукового розпилювального піролізу на кремнієві підкладки р-типу. Гетероструктури були відпалені при 450°C для покращення кристалічності та міжфазного контакту. Електрична характеристика за допомогою вольт-амперних вимірювань виявила чітку біполярну РС-поведінку без необхідності початкового процесу формування. Пристрої демонстрували стабільний стан високого опору (HRS) та стан низького опору (LRS) протягом кількох циклів, зі співвідношенням увімкнення/вимкнення, що перевищує 10<sup>2</sup>. Механізм перемикачання пояснюється утворенням та розривом провідних ниток, ймовірно, викликаних вакансіями кисню на межі розділу SnO<sub>2</sub>/ZnO. Оцінка ширини забороненої зони за допомогою графіків Таука показала значення приблизно 3,17 eV та 3,41 eV для ZnO та SnO<sub>2</sub> відповідно. Ці результати підтверджують потенціал гетеропереходів SnO<sub>2</sub>/ZnO як ефективних матеріалів для застосування в енергонеалежній пам'яті наступного покоління.

**Ключові слова:** SnO<sub>2</sub>; ZnO; резистивне перемикачання; мемристор; тонкі плівки; гетероперехід; енергонеалежна пам'ять; кисневі вакансії